Title

The serine/threonine-protein kinase/endoribonuclease IRE1α protects the heart against pressure overload–induced heart failure

Journal

Journal of Biological Chemistry, 293(25)

ISSN

0021-9258

Authors

Steiger, DeAnna
Yokota, Tomohiro
Li, Jin
et al.

Publication Date

2018-06-01

DOI

10.1074/jbc.ra118.003448

Peer reviewed

The serine/threonine-protein kinase/endoribonuclease IRE1α protects the heart against pressure overload–induced heart failure

Received for publication, April 14, 2018, and in revised form, May 4, 2018 Published, Papers in Press, May 16, 2018, DOI 10.1074/jbc.RA118.003448

DeAnna Steiger[‡1,2], **Tomohiro Yokota**[‡1,3], **Jin Li**[‡], **Shuxun Ren**[‡], **Susumu Minamisawa**[§], **and Yibin Wang**[‡4]

From the [‡]*Departments of Anesthesiology, Physiology, and Medicine, David Geffen School of Medicine, UCLA, Los Angeles, California 90095 and the* [§]*Department of Cell Physiology, Jikei University School of Medicine, Tokyo 105-8461, Japan*

Edited by Wolfgang Peti

Heart failure is associated with induction of endoplasmic reticulum (ER) stress and the unfolded protein response (UPR). The serine/threonine protein kinase/endoribonuclease IRE1α is a key protein in ER stress signal transduction. IRE1α activity can induce both protective UPR and apoptotic downstream signaling events, but the specific role for IRE1α activity in the heart is unknown. A major aim of this study was to characterize the specific contribution of IRE1α in cardiac physiology and pathogenesis. We used both cultured myocytes and a transgenic mouse line with inducible and cardiomyocyte-specific IRE1α overexpression as experimental models to achieve targeted IRE1α activation. IRE1α expression induced a potent but transient ER stress response in cardiomyocytes and did not cause significant effects in the intact heart under normal physiological conditions. Furthermore, the IRE1α-activated transgenic heart responding to pressure overload exhibited preserved function and reduced fibrotic area, associated with increased adaptive UPR signaling and with blunted inflammatory and pathological gene expression. Therefore, we conclude that IRE1α induces transient ER stress signaling and confers a protective effect against pressure overload–induced pathological remodeling in the heart. To our knowledge, this report provides first direct evidence of a specific and protective role for IRE1α in the heart and reveals an interaction between ER stress signaling and inflammatory regulation in the pathologically stressed heart.

Cardiovascular diseases are the number one cause of mortality in the United States and worldwide (1). Treatments for heart failure remain elusive due to the complexity of etiology and our limited understanding of the underlying mechanisms. Protein homeostasis is critical to cellular health, and defects in protein synthesis, maturation, and turnover are implicated in many human diseases (2–5), including heart failure (6). Protein homeostasis in the ER[5] lumen is monitored and maintained by highly conserved quality control mechanisms (7). Disruptions to ER homeostasis, including altered redox status, calcium flux, protein aggregation, or accumulation of client proteins, cause ER stress and activation of a highly conserved unfolded protein response (UPR) (also known as ER stress response) (8–10). The UPR conveys stress from the ER to the nucleus (11, 12), culminating in activation of transcription factors to up-regulate shaperone molecules and to suppress protein synthesis, leading to restored ER homeostasis (13). There are three major ER stress sensors and signal transducers involved in UPR, including activating transcription factor 6 (ATF6), protein kinase-like ER kinase (PERK), and inositol-requiring 1 (IRE1). They act in concert to restore protein folding in the ER lumen by reducing the client protein folding load, while increasing protein folding capacities and enhancing protein degradation for misfolded peptides, through coordinated induction of chaperone genes and inhibition of protein synthesis (14–18).

In the heart, ER stress signaling is activated in response to a broad spectrum of myocardial injuries, including ischemia, ischemia/reperfusion, hypoxia, and mechanical overload (6, 8, 19–24). ER stress signaling is also implicated in metabolic remodeling in the diseased heart (25). However, it remains unclear whether ER stress signaling is protective or detrimental to the heart. Some studies suggest that ER stress contributes to myocyte apoptosis and heart failure (21, 22, 26, 27), whereas other reports indicate that it is cardioprotective (24, 28, 29). Different ER stress pathways appear to have specific roles in the heart. ATF6-mediated signaling has been identified as a highly protective pathway against ischemia/reperfusion injury (24) by inducing BiP and GRP94. Similarly, Xbp1, downstream of

This work was supported in part by National Institutes of Health Grants HL103205 and HL070079 (to Y. W.) and additional funding from the Ministry of Education, Culture, Sports, Science, and Technology of Japan (to S. M.), the Vehicle Racing Commemorative Foundation (to S. M.), The Jikei University Graduate Research Fund (to S. M.), and the MEXT Supported Program for the Strategic Research Foundation at Private Universities (to S. M.). The authors declare that they have no conflicts of interest with the contents of this article. The content is solely the responsibility of the authors and does not necessarily represent the official views of the National Institutes of Health.

[1] Both authors contributed equally to this work.

[2] Supported by National Institutes of Health Ruth L. Kirschstein National Research Service Award F31 AG038156.

[3] Supported by a UCLA-Waseda Brain Circulation fellowship award from the Japanese Ministry of Science and Technology.

[4] To whom correspondence should be addressed. E-mail: yibinwang@mednet.ucla.edu.

[5] The abbreviations used are: ER, endoplasmic reticulum; UPR, unfolded protein response; ATF6, activating transcription factor 6; PERK, protein kinase-like ER kinase; IRE1, inositol-requiring 1; ANF, atrial natriuretic factor; BNF, brain natriuretic factor; TNF, tumor necrosis factor; IL, interleukin; TM, tunicamycin; JNK, c-Jun N-terminal kinase; TAC, transverse aortic constriction; MAPK, mitogen-activated protein kinase; H&E, hematoxylin and eosin; NRVM, neonatal rat ventricular myocyte; BisTris, 2-[bis(2-hydroxyethyl) amino]-2-(hydroxymethyl)propane-1,3-diol; p-, phosphorylated; LVID, diastolic/systolic diameter in the left ventricle; LVPW, diastolic/systolic posterior wall thickness in the left ventricle; adv, adenovirus.

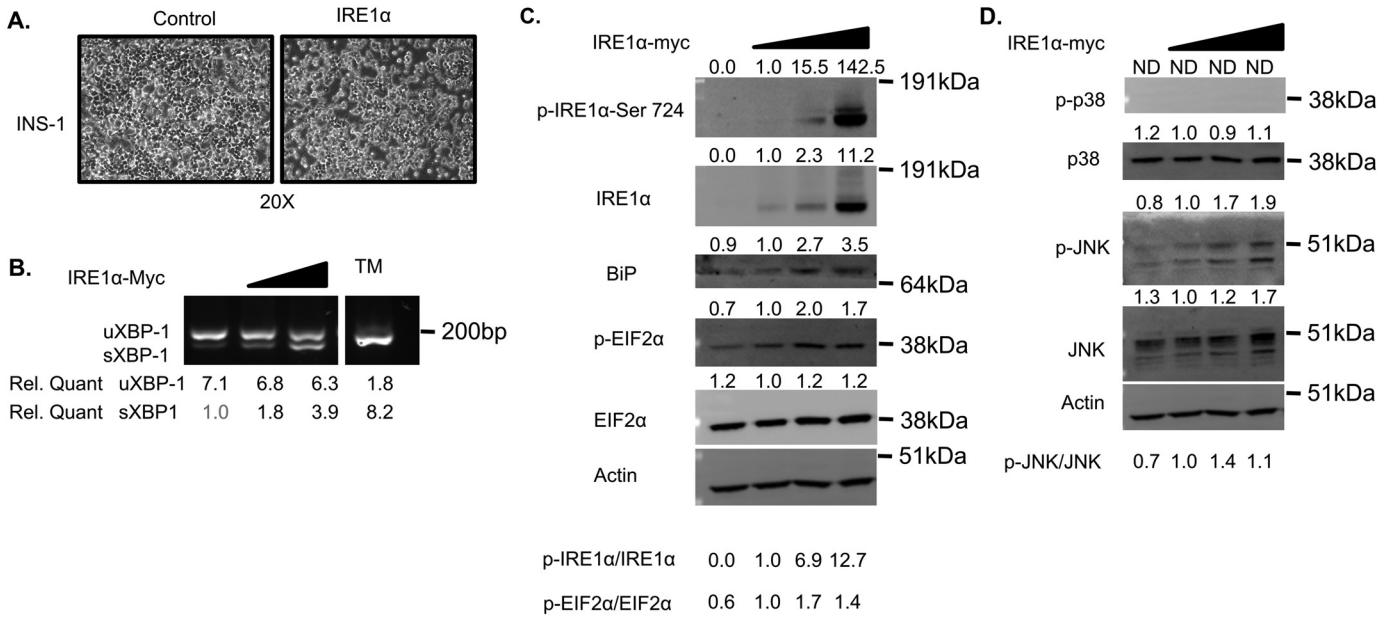

Figure 1. The functional impact of IRE1α activity in cells. *A*, representative images of adv-GFP– and adv-IRE1α–treated INS-1 cells. *B*, RT-PCR detection of spliced Xbp1 (*sXbp1*) levels in adv-IRE1α–treated INS-1 cells and quantification of the signal intensity as labeled. TM-treated cells are used as a positive control. *C*, immunoblots for the expression and autophosphorylation of IRE1α as well as ER stress–related proteins in adv-IRE1α–treated INS-1 cells and quantification of the signal intensity normalized by actin as *labeled*. *D*, immunoblots for stress-activated proteins p38 MAPK and JNK in adv-IRE1α–treated INS-1 cells and quantification of the signal intensity normalized by actin as *labeled*. *ND*, not detected.

IRE1α activation, was found to be protective against hypoxia and myocardial infarction also by inducing BiP (30) and coupling with hexosamine biosynthetic pathway (25). BiP expression can inhibit apoptotic signal CHOP and reduces apoptosis in cardiomyocytes (31). However, ER stress can also activate cell death signaling pathways (32–34). In particular, IRE1α binds to TRAF2 and activates downstream ASK1, resulting in JNK and p38 MAPK activation and apoptotic cell death (14, 35, 36). In contrast, other reports indicate that interactions between IRE1α and TRAF2 and JNK activate autophagy to promote cell survival during ER stress (37). PERK can also contribute to apoptotic signaling by promoting expression of ATF4 (17, 38, 39), a transcriptional activator for CHOP (40, 41). Angiotensin II, along with tunicamycin and thapsigargin, can induce both adaptive protein folding chaperones and apoptotic signal CHOP (6). ER stress can also induce hypertrophy gene expression, including atrial natriuretic factor (*ANF*) and brain natriuretic factor (*BNF*), suggesting that ER stress contributes to both adaptive and pathological remodeling. Finally, ER stress is implicated in cancer therapy Imatinib-induced cardiomyopathy (26). Although evidence is clear about the importance of ER stress regulation in cardiac pathogenesis, the specific contribution of IRE1-mediated signaling in the heart has not yet been directly investigated.

In the current study, we investigated the direct impact of IRE1α activation in the heart. In cardiomyocytes in culture, IRE1α overexpression induced significant IRE1α autophosphorylation and Xbp1 activation, as expected. However, there was no evidence of induction in cell death, stress signaling, or hypertrophy upon prolonged IRE1α expression. Using an animal model with heart-specific, tamoxifen-inducible IRE1α overexpression, we investigated the direct impact of IRE1α expression *in vivo*. Overexpression of IRE1α did not lead to any pathological phenotype at baseline. Following pressure overload induced by trans-aortic constriction, IRE1α expression in transgenic hearts showed better preserved function, blunted pathologic marker gene induction, and better preserved ER stress signaling. More interestingly, the expression of inflammatory cytokines TNFα and IL-6 was significantly blunted by IRE1α expression, suggesting that IRE1α-mediated ER stress signaling inhibits inflammatory cytokine induction in the heart. Thus, IRE1α activity has a direct protective effect in the heart against pressure overload–induced cardiac pathology, involving suppression of pro-inflammatory gene expression.

Results

IRE1α induces adaptive and transient UPR in cardiac myocytes

To investigate the functional impact of IRE1α activity, we generated adenoviral vectors expressing WT IRE1α. To validate the functionality of this expression vector, we tested the adenoviral vector in INS-1 cells. As shown in Fig. 1, IRE1α expression in INS-1 cells led to significant cell death 2 days after transfection (Fig. 1*A*). Xbp1 splicing was induced in a dose-dependent manner by IRE1α expression, similar to tunicamycin (TM) treatment (Fig. 1*B*). In addition, IRE1α autophosphorylation, BiP expression, phospho-EIF2α (Fig. 1*C*), and JNK kinase activity (Fig. 1*D*) were also induced in a dose-dependent fashion by IRE1α expression in INS-1 cells. These data are consistent with previous literature where IRE1α expression promotes cell death, associated with elevated RNase and stress kinase signaling via oligomerization in INS-1 cells (42, 43). In contrast, neonatal rat ventricular myocytes (NRVMs) with IRE1α overexpression did not show significant difference in morphology or cell sizes (Fig. 2*A*), although autophosphorylation and downstream Xbp1 activation were detected as in INS-1 cells (Fig. 2, *B*

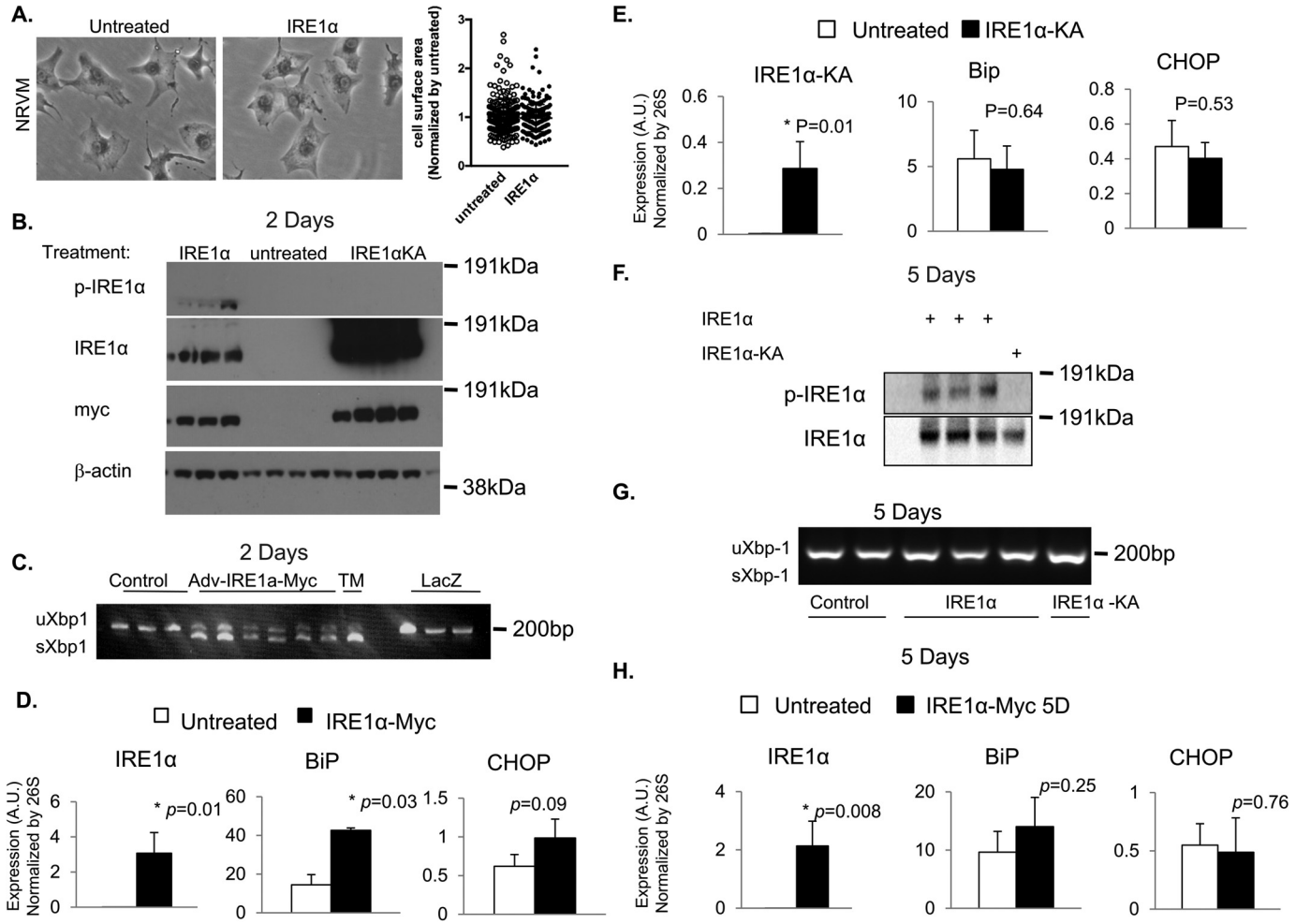

Figure 2. The functional impact of IRE1α activity on the cardiomyocyte. *A*, representative images of mock– and adv-IRE1α–treated NRVMs and cell-surface area. *B*, immunoblots of phospho-IRE1α, total IRE1α, Myc, and actin in NRVMs treated with mock, adv-IRE1α, and adv-IRE1αKA vectors 2 days post-transfection. *C*, RT-PCR detection of *sXbp1 versus uXbp1* levels in adv-IRE1α–treated NRVMs at 2 days post-transfection. *D*, quantitative measurements of mRNA for *IRE1α*, *BiP*, and *CHOP* in NRVMs treated with adv-IRE1α for 2 days. $n = 3$. *, $p < 0.05$. *E*, quantitative measurements of mRNA for *IRE1α*, *BiP*, and *CHOP* in NRVMs treated with adv-IRE1αKA for 2 days. $n = 3$. *, $p < 0.05$. *F*, immunoblots for phospho-IRE1α in NRVMs treated with adv-IRE1α or adv-IRE1αKA for 5 days. *G*, RT-PCR detection of sXbp1 levels in adv-IRE1α– or adv-IRE1αKA–treated NRVMs for 5 days. *H*, mRNA expression of *IRE1α*, *BiP*, and *CHOP* in NRVMs treated with adv-IRE1α for 5 days. $n = 3$. *A.U.*, arbitrary units; *error bars*, S.D.

and *C*). Other ER stress effectors, such as BiP expression, were also significantly induced by IRE1α overexpression, whereas the pro-apoptotic ER stress gene CHOP was not ($p = 0.09$) (Fig. 2*D*). As expected, expression of a kinase-dead IRE1α-KA mutant did not affect any of the ER stress molecules (Fig. 2*E*). These results revealed an unexpected myocyte-specific response to IRE1α expression, where only a subset of cytoprotective ER stress response was triggered in primary cardiomyocytes without activating the pro-apoptotic downstream pathway. Remarkably, prolonged IRE-1α expression (5 days) failed to sustain downstream Xbp1 activation or other UPR gene expression, although IRE1α autophosphorylation remained elevated (Fig. 2, *F–H*). These observations have revealed two specific features in IRE1α function in cardiomyocytes; one is a selective induction of IRE1α-mediated cytoprotective response *versus* stress signaling, and another involves the transient nature of the IRE1α-induced downstream Xbp1 activation, most likely due to a yet to be identified negative feedback inhibition.

Heart-specific and inducible expression of IRE1α in mice

To elucidate IRE1α function in intact heart, we generated an animal model where IRE1α expression was both inducible and heart-specific using a Cre-loxP–mediated gene switch strategy (Fig. 3*A*) (44). Cre-dependent expression of IRE1α was demonstrated in 293 cells, validating the efficacy of the construct (Fig. 3*B*). As shown *in vitro*, the Flox-GFP-IRE1α transgenic mice showed widespread expression of GFP but not the IRE1α transgene. After cross-breeding with αMHC-Mer-Cre-Mer mice (45–47), the transgenic gene IRE1α was induced only in ventricular tissue only after tamoxifen treatment (Fig. 3, *C–E*). Four weeks after transgene induction, no abnormal phenotype was observed in the IRE1α-expressing hearts compared with the littermate controls, including non-transgenic or single-transgenic mice, based on morphometric, histological, and functional analysis (Fig. 4). Furthermore, mRNA levels of *sXbp1*, *BiP*, and *CHOP* (Fig. 5*A*) were not affected by IRE1α expression, consistent with our *in vitro* observation after long-term IRE1α expression. The molecular profiles of *ANF*,

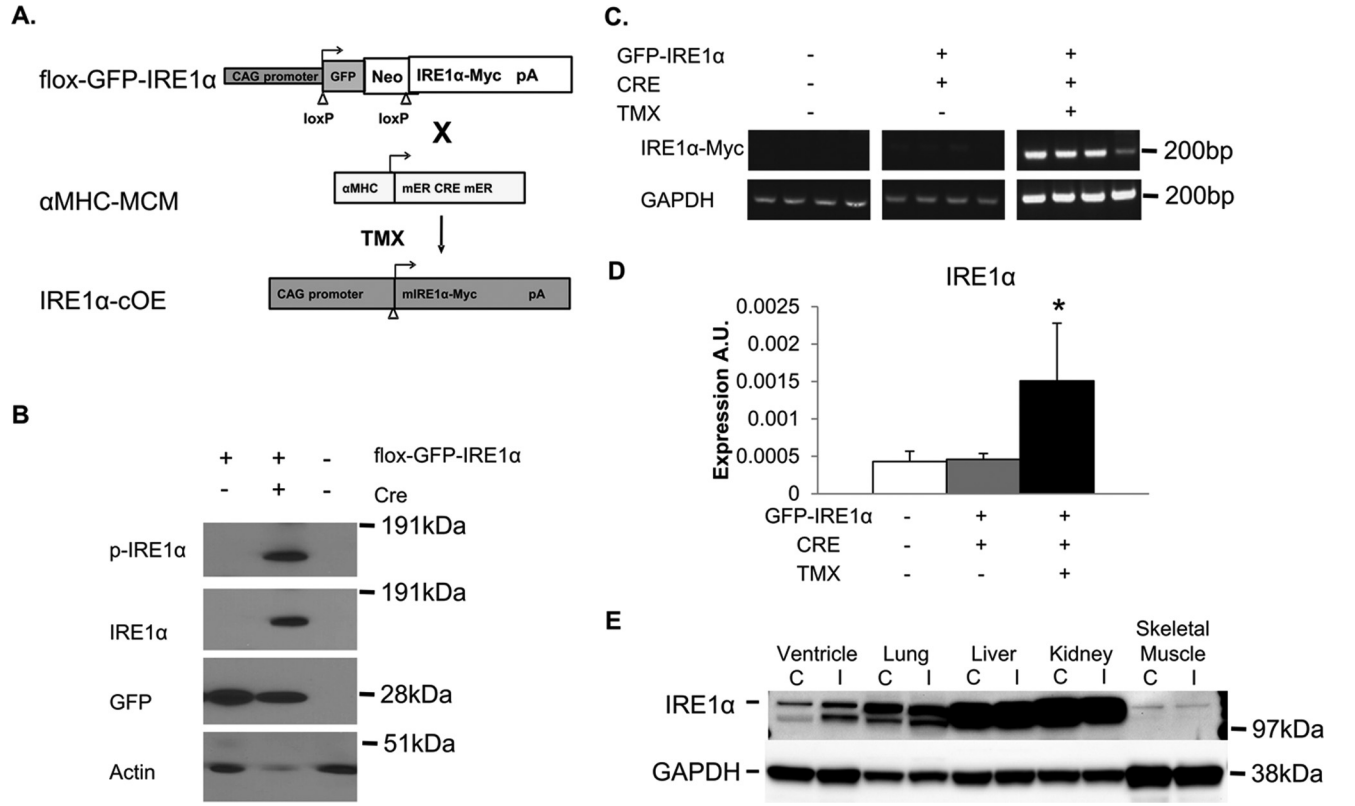

Figure 3. Establishment of IRE1α transgenic mouse line. *A*, *schematic diagram* for cardiac-specific inducible IRE1α transgenic construct and expected Cre/Lopx-mediated deletion. *B*, immunoblots of phospho-IRE1α, total IRE1α, GFP, and actin in HEK293 cells transfected with flox-GFP-IREα vector. *C*, representative RT-PCR detection of *IRE1α* expression in different transgenic ventricular tissues from control (Cre−/GFP−IREα−) and IRE1α transgenic (Cre+/GFP−IREα+) hearts, with or without tamoxifen (*TMX*) treatment. *D*, quantification of *IRE1α* mRNA expression in heart tissue from the same cohorts as in *C*. *E*, immunoblots of total IRE1α and glyceraldehyde-3-phosphate dehydrogenase (*GAPDH*) in ventricle, lung, liver, kidney, and skeletal muscle from control (*C*) and IRE1α transgenic (*I*) mice. *A.U.*, arbitrary units; *error bars*, S.D.

β-MHC, and *TNFα* were all unchanged following IRE1α overexpression (Fig. 5*B*). Together, these observations suggest that IRE1α expression was not sufficient to sustain ER stress response and did not exert any detrimental effect in the adult mouse heart.

IRE1α preserves heart function after transverse aortic constriction (TAC)

To test the effect of IRE1α expression on pathological stress response in heart, IRE1α transgenic mice were subjected to pressure overload implemented by TAC (48, 49). Pressure overload led to significant loss of cardiac function over time in the control mice. In contrast, the IRE1α transgenic mice demonstrated preserved function even at 4 weeks post-TAC (Fig. 6*A*), associated with reduced chamber dilation at the systole (Fig. 6*B*) based on echocardiograph measurements. Furthermore, the induction of pathological marker genes, including *ANF* and *βMHC*, was significantly blunted in response to TAC in the IRE1α transgenic heart *versus* the controls (Fig. 6*C*). However, cardiac hypertrophy as measured from tissue weight and histology was induced by TAC to the same levels in the control *versus* the IRE1α transgenic hearts (Fig. 6, *D* and *E*). Interestingly, fibrotic induction in myocardium was also significantly blunted in response to TAC in the IRE1α transgenic heart *versus* the controls (Fig. 6, *E* and *F*).

To investigate the potential mechanism, we analyzed the expression of UPR genes and stress-signaling molecules in post-TAC hearts. Although there was a trend for lower *BiP* expression in the post-TAC hearts, the IRE1α heart showed a modestly but significantly higher level of *BiP* expression than controls after TAC (Fig. 7*A*). In contrast, the mRNA level of *CHOP* was not affected by IRE1α expression, whereas there was trend for lower expression of *ATF4* in the post-TAC IRE1α transgenic heart (38) (Fig. 7*A*). Therefore, IRE1α expression in the heart leads to better preserved heart function following the TAC with only modest impact on ER stress downstream molecules. ER stress signaling by IRE1α and TRAF2 has been reported to activate inflammatory signals (50). As shown in Fig. 7*B*, IRE1α transgenic hearts showed significantly reduced TAC-induced mRNA expression for both *TNFα* and *IL-6* cytokines after comparing with the controls. Furthermore, whereas NF-κB induction was not affected by IRE1α expression in the post-TAC hearts, the IkB kinase β induction was significantly blunted in the IRE1α transgenic hearts, suggesting that attenuated NF-κB signaling may in part contribute to reduced *TNFα*/*IL-6* induction in the IRE1α TAC heart. In summary, IRE1α expression in the heart protects cardiac dysfunction associated with blunted induction of pro-inflammatory genes.

Discussion

This study provided first comprehensive characterization of the specific function of IRE1α as one of the three major ER stress-signaling branches in pressure overload–induced cardiac remodeling and dysfunction. In cultured cardiomyocytes,

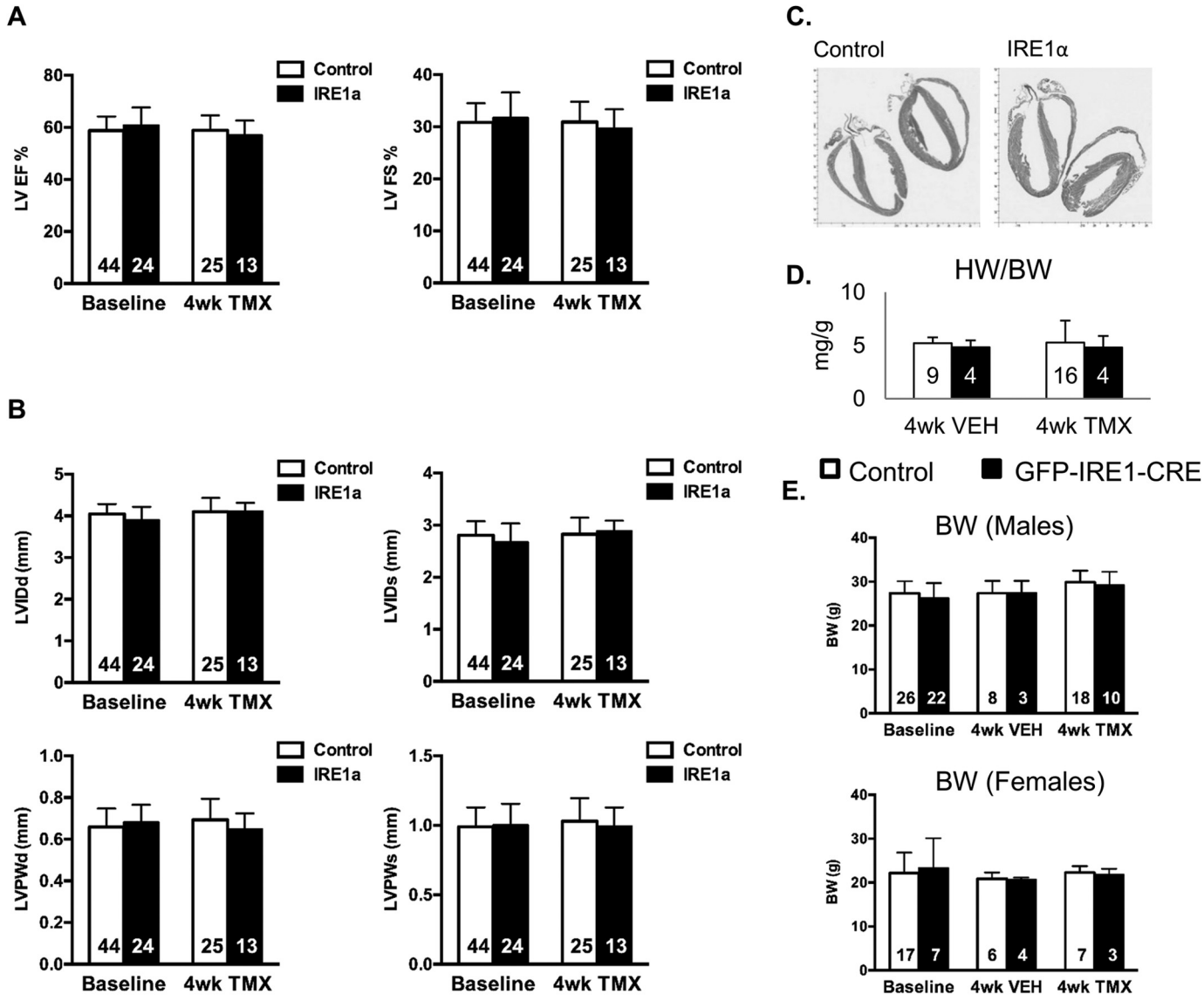

Figure 4. Characterization of IRE1α transgenic mouse heart at basal conditions. *A*, echocardiogram analysis of ejection fraction (*EF*) and fractional shortening (*FS*) in the IRE1α transgenic and control mice. *B*, echocardiogram analysis of diastolic/systolic diameter in the left ventricle (LVID) and diastolic/systolic posterior wall thickness in the ventricle (LVPW). *C*, representative image of H&E-stained hearts from IRE1α transgenic and control mice. *D*, heart weight/body weight ratio in IRE1α transgenic and control mice. *E*, body weights 4 weeks after vehicle or tamoxifen injection in both male and female mice. *Error bars*, S.D.

we observed transient induction of canonical Xbp1 activation following IRE1α expression without significant effects on cell death and hypertrophy. In intact heart, IRE1α expression did not affect pressure overload–induced cardiac hypertrophy but significantly attenuated cardiac dysfunction and pathological marker gene expression. Interestingly, IRE1α expression markedly blunted the induction of pro-inflammatory cytokine gene expression following TAC. Therefore, our results provide direct *in vitro* and *in vivo* evidence that IRE1α-mediated signaling is cardioprotective, at least in the setting of pressure overload–induced cardiac dysfunction.

ER stress-signaling pathways and the ensuing unfolded protein response are important cellular responses to various insults and have been found to be activated in human congestive heart failure (6), ischemic heart disease (21), and heart failure in response to the cancer drug imatinib (26). Experimental models have also recapitulated these observations (6, 24), but it is unclear whether ER stress signaling plays protective (24, 30, 31) or pathological roles in heart (22, 26, 51, 52). Expression of a constitutively active ATF6 shows a strong protection against ischemia reperfusion injury in mice (24). CHOP inhibition in NRVMs was also protective against apoptosis in the setting of ER stress by proteasome inhibition (31), and CHOP inactivation *in vivo* protected mouse hearts against apoptosis following ischemia/reperfusion injury (52). Among the three major UPR pathways (*i.e.* IRE1, PERK, and ATF6), IRE1 is unique in terms of diverse downstream outcome. IRE1 activation is capable of both protective and apoptotic signaling through Xbp1 or TRAF2 and stress-activated MAPK signaling cascades, respectively, as demonstrated previously (14, 18, 42, 43, 53, 54) (Fig. 1). However, the molecular nature of IRE1α function and regulation appears to be highly cell type–specific. Whereas constitu-

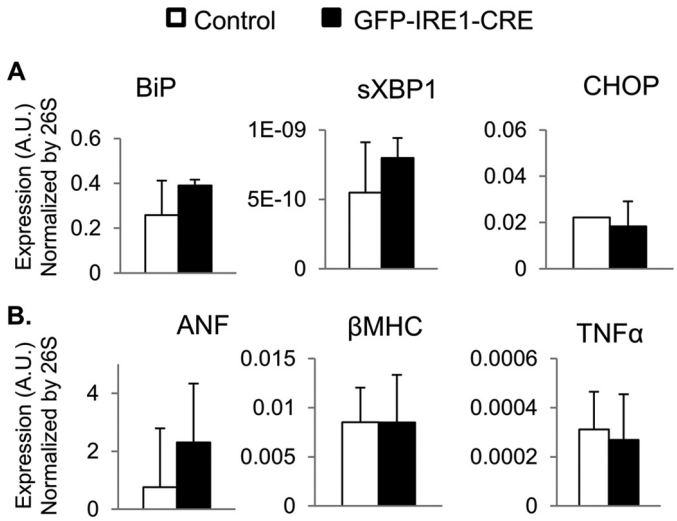

Figure 5. ER stress, hypertrophic, and inflammatory gene expression in IRE1α transgenic mouse heart at basal conditions. *A*, mRNA levels of ER stress–related gene *BiP*, *sXbp1*, and *CHOP* expression in IRE1α transgenic *versus* control mouse heart at basal conditions. *B*, hypertrophic markers *ANF* and *βMHC* and inflammatory gene *TNFα* expression in IRE1α transgenic *versus* control mouse heart at basal conditions. $n = 3$. *A.U.*, arbitrary units; *error bars*, S.D.

tive expression of IRE1α led to cell death in nonmyocytes, such as INS-1 cells (42), as well as other cell types (54), similar expression in cardiomyocytes achieved only transient induction of Xbp1 but without cell death induction. More remarkably, prolonged expression led to sustained autophosphorylation of IRE1α in cardiomyocytes, but only transient induction of *Xbp1*, suggesting the presence of a negative inhibitory feedback mechanism for IRE1 signaling in cardiomyocytes. It is well established that the RNase activity of IRE1 is induced by oligomerization and trans-molecular autophosphorylation (55). However, its inhibition is poorly characterized but may involve Bax inhibitor 1 (56), Hsp90–Cdc37 complex (57), or an ER-specific protein phosphatase (PP2Ce) (58). In cardiomyocytes, *Xbp1*-splicing activity is attenuated over time, whereas the IRE1α phosphorylation level remains elevated, suggesting that the underlying molecular mechanism may involve uncoupling of its autophosphorylation status and the *Xbp1*-splicing activity. The molecular basis of such negative feedback regulation should be further studied.

We observed that IRE1α transgenic mice had preserved heart function in response to pressure overload. The underlying mechanism is yet to be uncovered. It is known that inflammatory cytokines are induced in stressed myocardium, contrib-

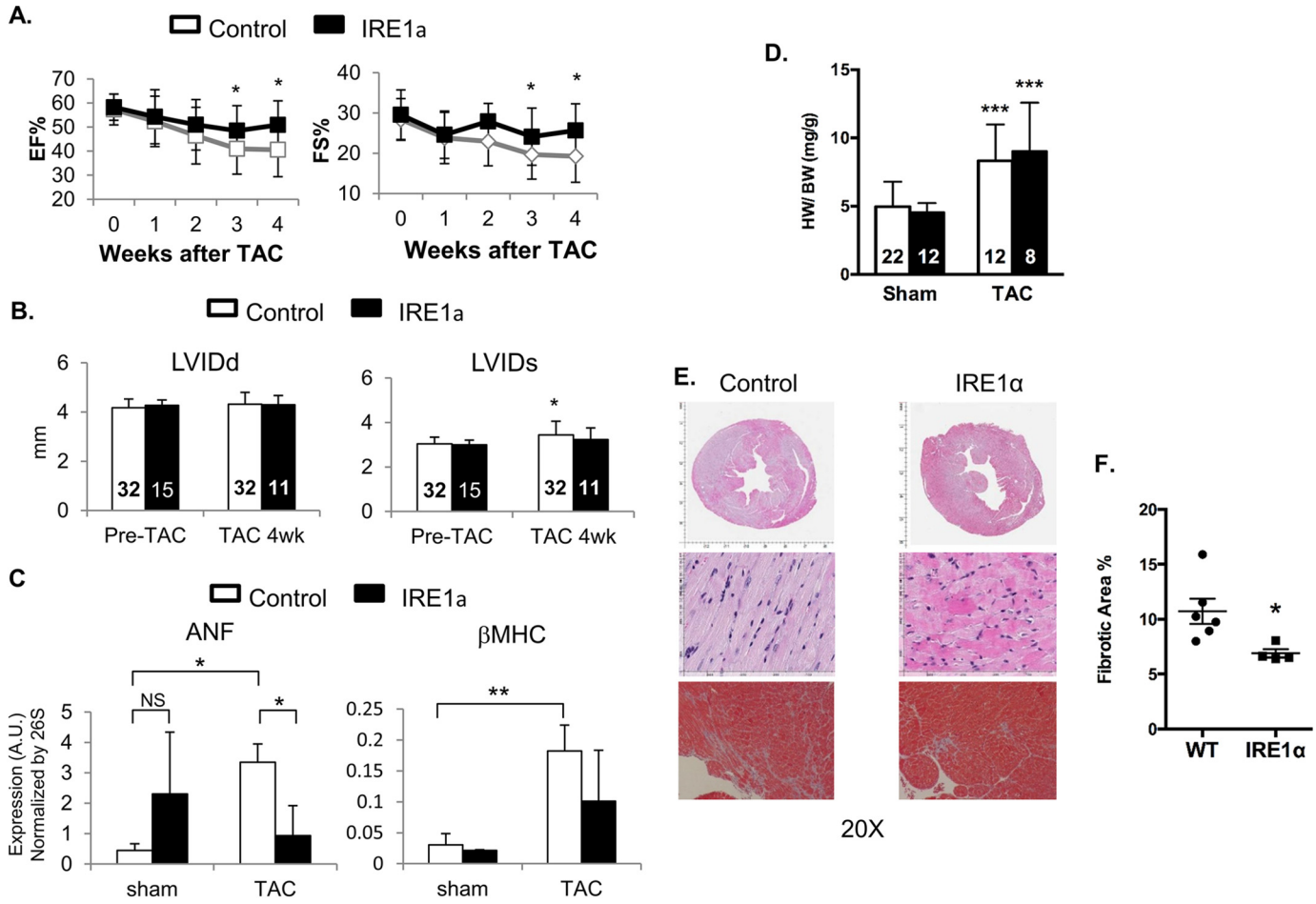

Figure 6. Preservation of cardiac function in IRE1α transgenic heart in response to pressure overload. *A*, echocardiogram analysis of EF and FS in the IRE1α transgenic *versus* control mouse after TAC. *, $p < 0.05$. *B*, echocardiogram analysis of diastolic/systolic LVID and diastolic/systolic LVPW 4 weeks post-TAC. *, $p < 0.05$. *C*, hypertrophic marker *ANF* and *βMHC* expression after 4 weeks post-TAC. *, $p < 0.05$. $n = 3–4$. *D*, heart weight/body weight in IRE1α transgenic and control mice 4 weeks post-TAC. ***, $p < 0.001$. *E*, representative image of H&E staining and trichrome staining in IRE1α transgenic and control mice 4 weeks post-TAC. *F*, quantification results of fibrotic area in IRE1α transgenic and control mice 4 weeks post-TAC. *, $p < 0.05$. $n = 4–6$. *A.U.*, arbitrary units; *error bars*, S.D.

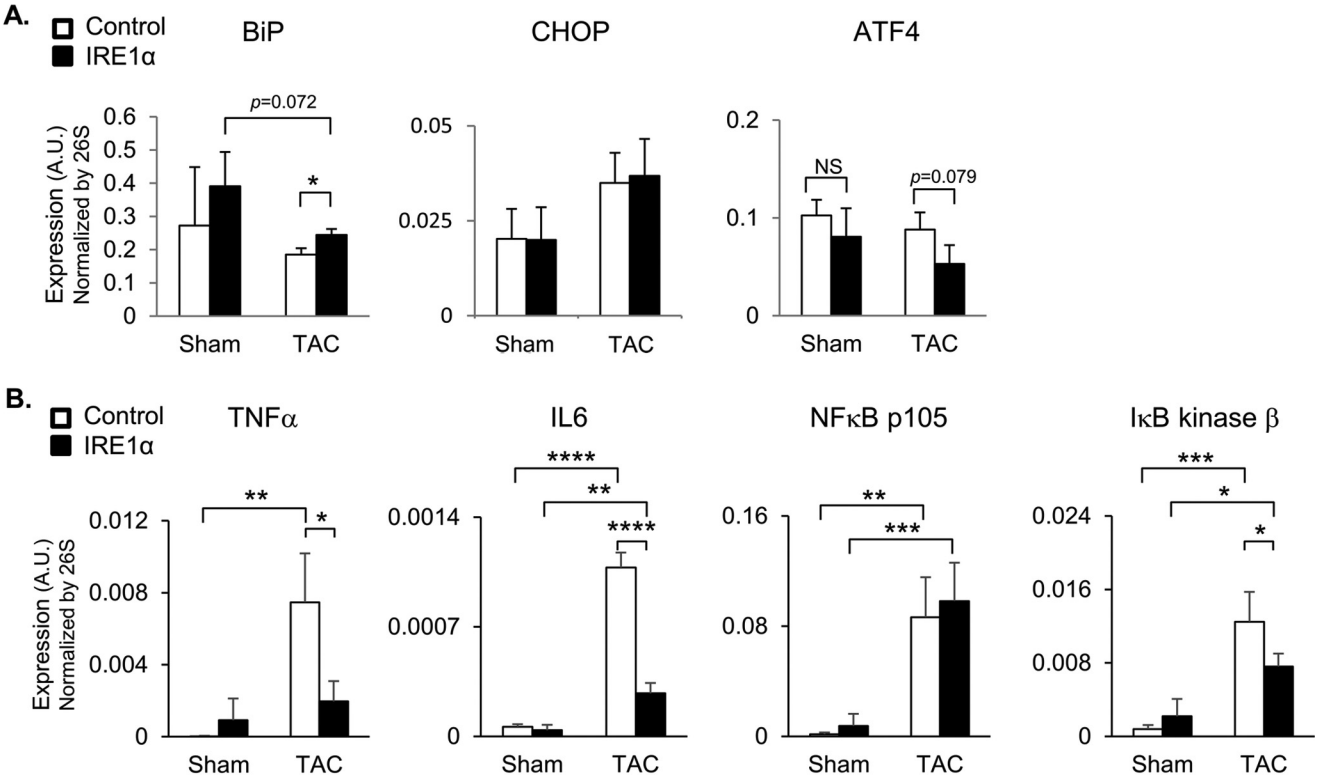

Figure 7. ER stress and inflammatory gene expression in IRE1α transgenic mouse heart in response to pressure overload. *A*, ER stress marker *BiP*, *CHOP*, and *αTF4* mRNA expression. *, $p < 0.05$. $n = 3–4$. *B*, mRNA levels of inflammatory genes *TNFα* and *IL-6* and NF-κB signaling genes *NFκB* and *IkB kinase β* in control and IRE1α transgenic hearts following sham or pressure overload. ****, $p < 0.0001$; ***, $p < 0.001$; **, $p < 0.01$; *, $p < 0.05$. $n = 3–4$. *A.U.*, arbitrary units; *error bars*, S.D.

uting to cardiac dysfunction and pathological remodeling. Indeed, both *TNFα* and *IL-6* expressions were markedly reduced in the post-TAC IRE1α transgenic hearts. It is reported that both *TNFα* and *IL-6* are induced by stress signaling, such as p38 MAPK (59, 60) and NF-κB pathway. Although we did not observe any effects on p38 activation, *IKKβ* induction was significantly attenuated by IRE1α expression. The data are consistent with the notion that IRE1α expression in cardiomyocytes promotes cytoprotective ER stress signaling but not downstream stress signaling and offer a potential mechanistic link between ER stress signaling and anti-inflammatory gene induction in pathologically stressed myocardium. Establishing the cardioprotective role of IRE1α in the intact heart illustrates the potential contribution of ER stress signaling to the pathogenesis of heart failure as well as the feasibility of targeted manipulation of ER stress signaling for treating the disease.

Experimental procedures

Animal models and surgical procedures

The investigation conformed with the Guide for the Care and Use of Laboratory Animals published by the National Institutes of Health (Publication number 85-23, revised 1985). All procedures were performed in accordance with UCLA animal welfare guidelines and approved by the UCLA institutional animal care and use committee. IRE1α was cloned into a vector for generation of transgenic animals with Cre-regulated expression of the transgene of interest (61, 62). Transgenic animals were generated in C57/Bl6 background through collaboration with the UCLA Molecular Genetics Technology Center. Founder animals were identified by PCR with transgene-specific primers.

Animals with heart-specific, inducible IRE1α overexpression were generated by crossing transgenic founder animals with previously established αMHC-Mer-Cre-Mer (MCM) transgenic mice (47) (45). IRE1α transgene overexpression was induced by intraperitoneal injection of tamoxifen citrate salt (Sigma), 20 mg/kg body weight/day for 5 days (45). WT and floxed single-transgenic littermate animals treated with tamoxifen or double-transgenic flox-GFP/CRE animals treated with vehicle were also used as controls. Both male and female mice age 12–16 weeks were included in this study.

TAC was performed as described previously with modifications (49). Mice were anesthetized with ketamine (80 mg/kg)/xylazine (20 mg/kg) by intraperitoneal injection. Respiration was provided by mechanical ventilation with 95% O_2 (tidal volume 0.5 ml, 130 breaths/min). Left parasternal thoracotomy was performed to access the transverse aorta, which was tied with a 5-0 nylon suture on a 27-gauge needle. The needle was removed, leaving in place a 65–70% constriction of the aortic lumen. Constriction of the aorta was confirmed by measuring differential blood flow through the right and left carotid arteries 1 week after surgery.

Animals were continuously anesthetized with 1.5% isoflurane and 95% oxygen. VisualSonics Vevo 770 and Vevo 2100 imaging systems and a 30-mHz scan head (Toronto, Canada) were used to collect short and long axis B-mode and M-mode

views. Reported values refer to short-axis measurements and calculations.

Histology

Hearts were perfused and fixed in 10% formalin before embedding in paraffin. All short-axis sections were prepared from mid-ventricle. Sections of 4-μm heart were deparaffinized and rehydrated before staining by hematoxylin and eosin (H&E) or Masson trichrome and Verhoeff–Van Gieson stain. Stained tissue sections were recorded as digital images by the Aperio XT whole-slide scanning system, and snapshot images were taken using the ImageScope software (Aperio Technologies, Vista, CA).

Cell culture

293 cells were maintained in Dulbecco's modified Eagle's medium supplemented with 10% fetal bovine serum (FBS) and 1% penicillin/streptomycin. Lipofectamine reagent (Life Technologies, Inc.) was used according to the manufacturer's protocol to achieve overexpression of the flox-GFP-IRE1α construct. INS-1 cells were cultured in RPMI1640 according to published methods (57). NRVMs were harvested from 1–3-day-old Sprague–Dawley rat pups as described previously (63) and cultured in serum-free Dulbecco's modified Eagle's medium supplemented with 1% penicillin/streptomycin and 1× Insulin-Transferrin-Selenium (ITS). NRVMs were infected with adenovirus (multiplicity of infection of 10) and incubated for 2 days before additional treatment with 5 g/ml TM for 4 h. Experiments with prolonged IRE1α expression were incubated for 5 days before RNA or protein analysis.

Western blotting

Cells were harvested for protein analysis with standard lysis buffer containing 1% Triton X-100, 1 mM β-glycerophosphate, 2.5 mM $Na_4P_2O_7$, 20 mM NaF, 1 mM Na_3VO_4, 1 mM phenylmethylsulfonyl fluoride, and protease inhibitor mixture (Roche Applied Science). Proteins were boiled for 5 min in LDS loading buffer containing 0.1% β-mercaptoethanol and separated on a 4–12% BisTris SDS-PAGE (Life Technologies). Specific proteins were detected with antibodies directed against p-IRE1α (Novus Bio), IRE1α, actin (Santa Cruz Biotechnology), BiP/Grp78 (Stressgen), p-p38, p38, p-JNK, JNK, p-IEF2α, eIF2α, GFP, and CHOP (Cell Signaling Technologies), as shown in Table 1.

RNA and RT-PCR analysis

Total RNA was isolated from heart or cells with TRIzol (Life Technologies). For animal studies, cDNA was prepared using iScript Reverse Transcription Supermix and amplified with SsoFast EvaGreen Supermix on a CVX96 thermal cycler (all from Bio-Rad). For cell studies, cDNA was prepared using Superscript II (Invitrogen) and amplified with SYBR Green supermix on a MyIQ system (Bio-Rad). Melt curves were generated for each primer set during each experiment, and analysis was performed using the ΔΔ*CT* method (Table 2).

Xbp1 activation

IRE1α RNase activity toward *Xbp1* mRNA was monitored by semiquantitative PCR. Both unspliced and spliced *Xbp1* mRNA were amplified with primers targeting the region surrounding the IRE1α-dependent splicing site (forward, 5′-GTTCCAGAGGTGGAGGCCA-3′; reverse, 5′-CATGACAGGGTCC-

Table 1
Antibodies

Antibodies	Vendor	Catalog no.	Dilution
p-IRE1α (Ser-724)	Novus Bio	NB100-2323	1:1000
IRE1α	Santa Cruz Biotechnology	SC-20790	1:500
Actin	Santa Cruz Biotechnology	SC-1616	1:1000
CHOP	Santa Cruz Biotechnology	SC-7351	1:500
BiP/Grp78	Santa Cruz Biotechnology	SC-1050	1:500
p-p38	Cell Signaling	9211	1:1000
p38	Cell Signaling	9212	1:1000
p-JNK	Cell Signaling	9251	1:1000
JNK	Cell Signaling	9252	1:1000
p-eIF2α	Cell Signaling	9721	1:1000
eIF2α	Cell Signaling	9722	1:1000
GFP	Cell Signaling	2956	1:1000

Table 2
Primers

Target	Sequence	
	Forward	Reverse
For mouse		
Xbp1 Total	TGGACTCTGACACTGTTGCC	CTCTGGGGAAGGACATTTGA
sXbp1	CAGTGGTCGCCACCGTCCATC	TGCCGCGCCCAGCCTTTCTA
Xbp1 splicing	GTTCCAGAGGTGGAGGCCA	CATGACAGGGTCCAACTTGTCC
CHOP	TATCTCATCCCCAGGAAACG	GGGCACTGACCACTCTGTTT
BiP	GAGGCTGTAGCCTATGGTGC	TTTGTTAGGGGTCGTTCACC
Rps26	GCCTCTTTACATGGGCTTTG	GCCATCCATAGCAAGGTTGT
For mouse/rat		
IRE1α	ACGGTGGACATCTTTTCGC	TGGGGATCCATAGCAATCAT
IRE1α MYC	TCAGGAGACGCTGGGCTCCATC	AGAGATCAGCTTCTGCTCGCCTC
ANF	CTGATGGATTTCAAGAACCTGCT	CTCTGGGCTCCAATCCTGTC
βMHC	CTCAACTGGGAAGAGCATCCA	CCTTCAGCAAACTCTGGAGGC
TNFα	CTCTTCAAGGGACAAGGCTG	TGGAAGACTCCTCCCAGGTA
GAPDH	TCCTGCACCACCAACTGCTTAG	GATGACCTTGCCCACAGCCTTG
For rat		
RatXBP1	CTCAGAGGCAGAGTCCAAGG	ACAGGGTCCAACTTGTCCAG
sXBP1	TCTGCTGAGTCCGCAGCAGG	CTCTAAGACTAGAGGCTTGG
uXBP1	CAGACTACGTGCGCCTCTGC	CTTCTGGGTAGACCTCTGGG
CHOP	CCTTCACTACTCTTGACCTGC	CGCTCGTTCTCTTCAGCAAG
BIP	TTCCGCTCTACCATGAAACC	CTTATTGTTACGGTGGGCT
RPS26	GCGTCTTCGACGCTTACGTGC	ACCTCTTTACATGGGCTTTGGTGGA

AACTTGTCC-3′). Products were amplified with the cycling protocol of 95 °C for 30 s, followed by 35 cycles of 95 °C for 30 s, 60 °C for 30 s, and 72 °C for 25 s, followed by 72 °C for 10 min. PCR products were separated on 4% agarose gel.

Statistical analysis

Data are presented as mean ± S.D. Means of two groups were compared by two-tailed Student's *t* test. Means of more than two groups were compared by analysis of variance and Turkey post hoc test. Differences between groups were considered statistically significant when $p < 0.05$.

Author contributions—D. S., T. Y., J. L., and S. R. data curation; D. S. formal analysis; D. S., T. Y., S. R., and Y. W. investigation; D. S. writing-original draft; T. Y. validation; T. Y. and Y. W. methodology; T. Y., S. M., and Y. W. writing-review and editing; S. R., S. M., and Y. W. supervision; S. M. and Y. W. conceptualization; S. M. funding acquisition; Y. W. resources; Y. W. project administration.

Acknowledgment—We thank Haiying Pu for technical assistance.

References

1. Roger, V. L., Go, A. S., Lloyd-Jones, D. M., Benjamin, E. J., Berry, J. D., Borden, W. B., Bravata, D. M., Dai, S., Ford, E. S., Fox, C. S., Fullerton, H. J., Gillespie, C., Hailpern, S. M., Heit, J. A., Howard, V. J., *et al.* (2012) Heart disease and stroke statistics–2012 update: a report from the American Heart Association. *Circulation* **125,** e2–e220 CrossRef Medline
2. Lindholm, D., Wootz, H., and Korhonen, L. (2006) ER stress and neurodegenerative diseases. *Cell Death Differ.* **13,** 385–392 CrossRef Medline
3. Marciniak, S. J., and Ron, D. (2006) Endoplasmic reticulum stress signaling in disease. *Physiol. Rev.* **86,** 1133–1149 CrossRef Medline
4. Mitchell, S., Ota, A., Foster, W., Zhang, B., Fang, Z., Patel, S., Nelson, S. F., Horvath, S., and Wang, Y. (2006) Distinct gene expression profiles in adult mouse heart following targeted MAP kinase activation. *Physiol. Genomics* **25,** 50–59 CrossRef Medline
5. Ron, D., and Hubbard, S. R. (2008) How IRE1 reacts to ER stress. *Cell* **132,** 24–26 CrossRef Medline
6. Okada, K., Minamino, T., Tsukamoto, Y., Liao, Y., Tsukamoto, O., Takashima, S., Hirata, A., Fujita, M., Nagamachi, Y., Nakatani, T., Yutani, C., Ozawa, K., Ogawa, S., Tomoike, H., Hori, M., and Kitakaze, M. (2004) Prolonged endoplasmic reticulum stress in hypertrophic and failing heart after aortic constriction: possible contribution of endoplasmic reticulum stress to cardiac myocyte apoptosis. *Circulation* **110,** 705–712 CrossRef Medline
7. Ellgaard, L., and Helenius, A. (2003) Quality control in the endoplasmic reticulum. *Nat. Rev. Mol. Cell Biol.* **4,** 181–191 CrossRef Medline
8. Janero, D. R., Hreniuk, D., and Sharif, H. M. (1991) Hydrogen peroxide-induced oxidative stress to the mammalian heart-muscle cell (cardiomyocyte): lethal peroxidative membrane injury. *J. Cell. Physiol.* **149,** 347–364 CrossRef Medline
9. Schröder, M., and Kaufman, R. J. (2005) ER stress and the unfolded protein response. *Mutat. Res.* **569,** 29–63 CrossRef Medline
10. Bulleid, N. J. (2012) Disulfide bond formation in the mammalian endoplasmic reticulum. *Cold Spring Harb. Perspect. Biol.* **4,** a013219 CrossRef Medline
11. Mori, K., Kawahara, T., Yoshida, H., Yanagi, H., and Yura, T. (1996) Signalling from endoplasmic reticulum to nucleus: transcription factor with a basic-leucine zipper motif is required for the unfolded protein-response pathway. *Genes Cells* **1,** 803–817 CrossRef Medline
12. Tirasophon, W., Welihinda, A. A., and Kaufman, R. J. (1998) A stress response pathway from the endoplasmic reticulum to the nucleus requires a novel bifunctional protein kinase/endoribonuclease (Ire1p) in mammalian cells. *Genes Dev.* **12,** 1812–1824 CrossRef Medline
13. Shen, X., Zhang, K., and Kaufman, R. J. (2004) The unfolded protein response–a stress signaling pathway of the endoplasmic reticulum. *J. Chem. Neuroanat.* **28,** 79–92 CrossRef Medline
14. Urano, F., Wang, X., Bertolotti, A., Zhang, Y., Chung, P., Harding, H. P., and Ron, D. (2000) Coupling of stress in the ER to activation of JNK protein kinases by transmembrane protein kinase IRE1. *Science* **287,** 664–666 CrossRef Medline
15. Lee, A. S. (2005) The ER chaperone and signaling regulator GRP78/BiP as a monitor of endoplasmic reticulum stress. *Methods* **35,** 373–381 CrossRef Medline
16. Haze, K., Yoshida, H., Yanagi, H., Yura, T., and Mori, K. (1999) Mammalian transcription factor ATF6 is synthesized as a transmembrane protein and activated by proteolysis in response to endoplasmic reticulum stress. *Mol. Biol. Cell* **10,** 3787–3799 CrossRef Medline
17. Harding, H. P., Zhang, Y., and Ron, D. (1999) Protein translation and folding are coupled by an endoplasmic-reticulum-resident kinase. *Nature* **397,** 271–274 CrossRef Medline
18. Shamu, C. E., and Walter, P. (1996) Oligomerization and phosphorylation of the Ire1p kinase during intracellular signaling from the endoplasmic reticulum to the nucleus. *EMBO J.* **15,** 3028–3039 Medline
19. Glembotski, C. C. (2007) Endoplasmic reticulum stress in the heart. *Circ. Res.* **101,** 975–984 CrossRef Medline
20. Prins, D., and Michalak, M. (2009) Endoplasmic reticulum proteins in cardiac development and dysfunction. *Can. J. Physiol. Pharmacol.* **87,** 419–425 CrossRef Medline
21. Azfer, A., Niu, J., Rogers, L. M., Adamski, F. M., and Kolattukudy, P. E. (2006) Activation of endoplasmic reticulum stress response during the development of ischemic heart disease. *Am. J. Physiol. Heart Circ. Physiol.* **291,** H1411–H1420 CrossRef Medline
22. Terai, K., Hiramoto, Y., Masaki, M., Sugiyama, S., Kuroda, T., Hori, M., Kawase, I., and Hirota, H. (2005) AMP-activated protein kinase protects cardiomyocytes against hypoxic injury through attenuation of endoplasmic reticulum stress. *Mol. Cell. Biol.* **25,** 9554–9575 CrossRef Medline
23. Stadtman, E. R. (2004) Role of oxidant species in aging. *Curr. Med. Chem.* **11,** 1105–1112 CrossRef Medline
24. Martindale, J. J., Fernandez, R., Thuerauf, D., Whittaker, R., Gude, N., Sussman, M. A., and Glembotski, C. C. (2006) Endoplasmic reticulum stress gene induction and protection from ischemia/reperfusion injury in the hearts of transgenic mice with a tamoxifen-regulated form of ATF6. *Circ. Res.* **98,** 1186–1193 CrossRef Medline
25. Wang, Z. V., Deng, Y., Gao, N., Pedrozo, Z., Li, D. L., Morales, C. R., Criollo, A., Luo, X., Tan, W., Jiang, N., Lehrman, M. A., Rothermel, B. A., Lee, A. H., Lavandero, S., Mammen, P. P. A., *et al.* (2014) Spliced X-box binding protein 1 couples the unfolded protein response to hexosamine biosynthetic pathway. *Cell* **156,** 1179–1192 CrossRef Medline
26. Kerkelä, R., Grazette, L., Yacobi, R., Iliescu, C., Patten, R., Beahm, C., Walters, B., Shevtsov, S., Pesant, S., Clubb, F. J., Rosenzweig, A., Salomon, R. N., Van Etten, R. A., Alroy, J., Durand, J. B., and Force, T. (2006) Cardiotoxicity of the cancer therapeutic agent imatinib mesylate. *Nat. Med.* **12,** 908–916 CrossRef Medline
27. Cook, A. R., Bardswell, S. C., Pretheshan, S., Dighe, K., Kanaganayagam, G. S., Jabr, R. I., Merkle, S., Marber, M. S., Engelhardt, S., and Avkiran, M. (2009) Paradoxical resistance to myocardial ischemia and age-related cardiomyopathy in NHE1 transgenic mice: a role for ER stress? *J. Mol. Cell Cardiol.* **46,** 225–233 CrossRef Medline
28. Lynch, J. M., Maillet, M., Vanhoutte, D., Schloemer, A., Sargent, M. A., Blair, N. S., Lynch, K. A., Okada, T., Aronow, B. J., Osinska, H., Prywes, R., Lorenz, J. N., Mori, K., Lawler, J., Robbins, J., and Molkentin, J. D. (2012) A thrombospondin-dependent pathway for a protective ER stress response. *Cell* **149,** 1257–1268 CrossRef Medline
29. Briot, A., Jaroszewicz, A., Warren, C. M., Lu, J., Touma, M., Rudat, C., Hofmann, J. J., Airik, R., Weinmaster, G., Lyons, K., Wang, Y., Kispert, A., Pellegrini, M., and Iruela-Arispe, M. L. (2014) Repression of Sox9 by Jag1 is continuously required to suppress the default chondrogenic fate of vascular smooth muscle cells. *Dev. Cell* **31,** 707–721 CrossRef Medline
30. Thuerauf, D. J., Marcinko, M., Gude, N., Rubio, M., Sussman, M. A., and Glembotski, C. C. (2006) Activation of the unfolded protein response in

infarcted mouse heart and hypoxic cultured cardiac myocytes. *Circ. Res.* **99,** 275–282 CrossRef Medline
31. Fu, H. Y., Minamino, T., Tsukamoto, O., Sawada, T., Asai, M., Kato, H., Asano, Y., Fujita, M., Takashima, S., Hori, M., and Kitakaze, M. (2008) Overexpression of endoplasmic reticulum-resident chaperone attenuates cardiomyocyte death induced by proteasome inhibition. *Cardiovasc. Res.* **79,** 600–610 CrossRef Medline
32. Groenendyk, J., and Michalak, M. (2005) Endoplasmic reticulum quality control and apoptosis. *Acta Biochim. Pol.* **52,** 381–395 Medline
33. Kadowaki, H., Nishitoh, H., and Ichijo, H. (2004) Survival and apoptosis signals in ER stress: the role of protein kinases. *J. Chem. Neuroanat.* **28,** 93–100 CrossRef Medline
34. Kim, R., Emi, M., Tanabe, K., and Murakami, S. (2006) Role of the unfolded protein response in cell death. *Apoptosis* **11,** 5–13 CrossRef Medline
35. Zhang, C., Kawauchi, J., Adachi, M. T., Hashimoto, Y., Oshiro, S., Aso, T., and Kitajima, S. (2001) Activation of JNK and transcriptional repressor ATF3/LRF1 through the IRE1/TRAF2 pathway is implicated in human vascular endothelial cell death by homocysteine. *Biochem. Biophys. Res. Commun.* **289,** 718–724 CrossRef Medline
36. Hetz, C., Bernasconi, P., Fisher, J., Lee, A. H., Bassik, M. C., Antonsson, B., Brandt, G. S., Iwakoshi, N. N., Schinzel, A., Glimcher, L. H., and Korsmeyer, S. J. (2006) Proapoptotic BAX and BAK modulate the unfolded protein response by a direct interaction with IRE1alpha. *Science* **312,** 572–576 CrossRef Medline
37. Ogata, M., Hino, S., Saito, A., Morikawa, K., Kondo, S., Kanemoto, S., Murakami, T., Taniguchi, M., Tanii, I., Yoshinaga, K., Shiosaka, S., Hammarback, J. A., Urano, F., and Imaizumi, K. (2006) Autophagy is activated for cell survival after endoplasmic reticulum stress. *Mol. Cell. Biol.* **26,** 9220–9231 CrossRef Medline
38. Blais, J. D., Filipenko, V., Bi, M., Harding, H. P., Ron, D., Koumenis, C., Wouters, B. G., and Bell, J. C. (2004) Activating transcription factor 4 is translationally regulated by hypoxic stress. *Mol. Cell. Biol.* **24,** 7469–7482 CrossRef Medline
39. Zhang, K., and Kaufman, R. J. (2004) Signaling the unfolded protein response from the endoplasmic reticulum. *J. Biol. Chem.* **279,** 25935–25938 CrossRef Medline
40. Oyadomari, S., and Mori, M. (2004) Roles of CHOP/GADD153 in endoplasmic reticulum stress. *Cell Death Differ.* **11,** 381–389 CrossRef Medline
41. Zinszner, H., Kuroda, M., Wang, X., Batchvarova, N., Lightfoot, R. T., Remotti, H., Stevens, J. L., and Ron, D. (1998) CHOP is implicated in programmed cell death in response to impaired function of the endoplasmic reticulum. *Genes Dev.* **12,** 982–995 CrossRef Medline
42. Ghosh, R., Wang, L., Wang, E. S., Perera, B. G., Igbaria, A., Morita, S., Prado, K., Thamsen, M., Caswell, D., Macias, H., Weiberth, K. F., Gliedt, M. J., Alavi, M. V., Hari, S. B., Mitra, A. K., *et al.* (2014) Allosteric inhibition of the IRE1alpha RNase preserves cell viability and function during endoplasmic reticulum stress. *Cell* **158,** 534–548 CrossRef Medline
43. Han, D., Lerner, A. G., Vande Walle, L., Upton, J. P., Xu, W., Hagen, A., Backes, B. J., Oakes, S. A., and Papa, F. R. (2009) IRE1α kinase activation modes control alternate endoribonuclease outputs to determine divergent cell fates. *Cell* **138,** 562–575 CrossRef Medline
44. Ishikawa, T. O., and Herschman, H. R. (2006) Conditional knockout mouse for tissue-specific disruption of the cyclooxygenase-2 (Cox-2) gene. *Genesis* **44,** 143–149 CrossRef Medline
45. Sohal, D. S., Nghiem, M., Crackower, M. A., Witt, S. A., Kimball, T. R., Tymitz, K. M., Penninger, J. M., and Molkentin, J. D. (2001) Temporally regulated and tissue-specific gene manipulations in the adult and embryonic heart using a tamoxifen-inducible Cre protein. *Circ. Res.* **89,** 20–25 CrossRef Medline
46. Hayashi, S., and McMahon, A. P. (2002) Efficient recombination in diverse tissues by a tamoxifen-inducible form of Cre: a tool for temporally regulated gene activation/inactivation in the mouse. *Dev. Biol.* **244,** 305–318 CrossRef Medline
47. Petrich, B. G., Molkentin, J. D., and Wang, Y. (2003) Temporal activation of c-Jun N-terminal kinase in adult transgenic heart via cre-loxP-mediated DNA recombination. *FASEB J.* **17,** 749–751 CrossRef Medline
48. Rockman, H. A., Ross, R. S., Harris, A. N., Knowlton, K. U., Steinhelper, M. E., Field, L. J., Ross, J., Jr., and Chien, K. R. (1991) Segregation of atrial-specific and inducible expression of an atrial natriuretic factor transgene in an *in vivo* murine model of cardiac hypertrophy. *Proc. Natl. Acad. Sci. U.S.A.* **88,** 8277–8281 CrossRef Medline
49. Wang, Y., Huang, S., Sah, V. P., Ross, J., Jr., Brown, J. H., Han, J., and Chien, K. R. (1998) Cardiac muscle cell hypertrophy and apoptosis induced by distinct members of the p38 mitogen-activated protein kinase family. *J. Biol. Chem.* **273,** 2161–2168 CrossRef Medline
50. Hu, P., Han, Z., Couvillon, A. D., Kaufman, R. J., and Exton, J. H. (2006) Autocrine tumor necrosis factor α links endoplasmic reticulum stress to the membrane death receptor pathway through IRE1α-mediated NF-κB activation and down-regulation of TRAF2 expression. *Mol. Cell. Biol.* **26,** 3071–3084 CrossRef Medline
51. Isodono, K., Takahashi, T., Imoto, H., Nakanishi, N., Ogata, T., Asada, S., Adachi, A., Ueyama, T., Oh, H., and Matsubara, H. (2010) PARM-1 is an endoplasmic reticulum molecule involved in endoplasmic reticulum stress-induced apoptosis in rat cardiac myocytes. *PLoS One* **5,** e9746 CrossRef Medline
52. Miyazaki, Y., Kaikita, K., Endo, M., Horio, E., Miura, M., Tsujita, K., Hokimoto, S., Yamamuro, M., Iwawaki, T., Gotoh, T., Ogawa, H., and Oike, Y. (2011) C/EBP homologous protein deficiency attenuates myocardial reperfusion injury by inhibiting myocardial apoptosis and inflammation. *Arterioscler. Thromb. Vasc. Biol.* **31,** 1124–1132 CrossRef Medline
53. Zeng, L., Zampetaki, A., Margariti, A., Pepe, A. E., Alam, S., Martin, D., Xiao, Q., Wang, W., Jin, Z. G., Cockerill, G., Mori, K., Li, Y. S., Hu, Y., Chien, S., and Xu, Q. (2009) Sustained activation of XBP1 splicing leads to endothelial apoptosis and atherosclerosis development in response to disturbed flow. *Proc. Natl. Acad. Sci. U.S.A.* **106,** 8326–8331 CrossRef Medline
54. Wang, X. Z., Harding, H. P., Zhang, Y., Jolicoeur, E. M., Kuroda, M., and Ron, D. (1998) Cloning of mammalian Ire1 reveals diversity in the ER stress responses. *EMBO J.* **17,** 5708–5717 CrossRef Medline
55. Calfon, M., Zeng, H., Urano, F., Till, J. H., Hubbard, S. R., Harding, H. P., Clark, S. G., and Ron, D. (2002) IRE1 couples endoplasmic reticulum load to secretory capacity by processing the XBP-1 mRNA. *Nature* **415,** 92–96 CrossRef Medline
56. Lisbona, F., Rojas-Rivera, D., Thielen, P., Zamorano, S., Todd, D., Martinon, F., Glavic, A., Kress, C., Lin, J. H., Walter, P., Reed, J. C., Glimcher, L. H., and Hetz, C. (2009) BAX inhibitor-1 is a negative regulator of the ER stress sensor IRE1α. *Mol. Cell* **33,** 679–691 CrossRef Medline
57. Ota, A., and Wang, Y. (2012) Cdc37/Hsp90 protein-mediated regulation of IRE1α protein activity in endoplasmic reticulum stress response and insulin synthesis in INS-1 cells. *J. Biol. Chem.* **287,** 6266–6274 CrossRef Medline
58. Lu, G., Ota, A., Ren, S., Franklin, S., Rau, C. D., Ping, P., Lane, T. F., Zhou, Z. H., Reue, K., Lusis, A. J., Vondriska, T., and Wang, Y. (2013) PPM1l encodes an inositol requiring-protein 1 (IRE1) specific phosphatase that regulates the functional outcome of the ER stress response. *Mol. Metab.* **2,** 405–416 CrossRef Medline
59. Li, M., Georgakopoulos, D., Lu, G., Hester, L., Kass, D. A., Hasday, J., and Wang, Y. (2005) p38 MAP kinase mediates inflammatory cytokine induction in cardiomyocytes and extracellular matrix remodeling in heart. *Circulation* **111,** 2494–2502 CrossRef Medline
60. Yokota, T., and Wang, Y. (2016) p38 MAP kinases in the heart. *Gene* **575,** 369–376 CrossRef Medline
61. Liao, P., Georgakopoulos, D., Kovacs, A., Zheng, M., Lerner, D., Pu, H., Saffitz, J., Chien, K., Xiao, R. P., Kass, D. A., and Wang, Y. (2001) The *in vivo* role of p38 MAP kinases in cardiac remodeling and restrictive cardiomyopathy. *Proc. Natl. Acad. Sci. U.S.A.* **98,** 12283–12288 CrossRef Medline
62. Streicher, J. M., Ren, S., Herschman, H., and Wang, Y. (2010) MAPK-activated protein kinase-2 in cardiac hypertrophy and cyclooxygenase-2 regulation in heart. *Circ. Res.* **106,** 1434–1443 CrossRef Medline
63. Iwaki, K., Sukhatme, V. P., Shubeita, H. E., and Chien, K. R. (1990) α- and β-adrenergic stimulation induces distinct patterns of immediate early gene expression in neonatal rat myocardial cells: fos/jun expression is associated with sarcomere assembly; Egr-1 induction is primarily an α1-mediated response. *J. Biol. Chem.* **265,** 13809–13817 Medline